Available online at www.sciencedirect.com
SCIENCE DIRECT®
International Journal of Heat and Mass Transfer 47 (2004) 1771–1781
International Journal of HEAT and MASS TRANSFER
www.elsevier.com/locate/ijhmt

# Turbulent scalar transport mechanisms in plane channel and Couette flows

B. Debusschere *, C.J. Rutland

*Department of Mechanical Engineering, University of Wisconsin-Madison, 1500 Engineering Dr., Madison, WI 53706, USA*

Received 3 September 2002; received in revised form 15 October 2003

**Abstract**

To investigate the transport of scalars by turbulent flows with different shear stresses, direct numerical simulations were performed of passive heat transfer in a plane channel and Couette flow. The simulations showed that streamwise vortices play a significant role in near wall heat transfer for both flows. At the centerline, Couette flow has large scale structures that transport heat across the centerline. In channel flow, lower turbulence levels at the centerline are not effective in breaking up packets of hot or cold fluid. This results in higher temperature fluctuations at the centerline and overall lower heat transfer than in Couette flow.


## 1. Introduction

In the design of applications that involve mixing of fluids, such as a burner or an internal combustion engine, there is a need for accurate turbulent mixing models. Without an accurate prediction of heat and mass transfer fluxes, for example, it is impossible to correctly calculate the power and emissions output of combustion processes. To develop better turbulent heat and mass transfer models, a thorough understanding of turbulent transport is essential.

To gain more insight in turbulent transport processes, this study focuses on passive heat transfer as a special case of scalar transport. Two different flow configurations are compared: plane channel flow and plane Couette flow. The different velocity boundary conditions in these two flows lead to turbulence fields with different shear stress levels even though the geometries are the same. For both cases, the temperature boundary conditions are isothermal walls with the upper wall at a higher temperature than the lower wall. In this way, plane channel and Couette flows are viewed as canonical flows that represent aspects of more complex turbulent flow fields.

Channel and Couette flows have been studied extensively, both experimentally and numerically. Investigation of the near wall turbulence in both channel and Couette flows (as well as in boundary layers) has led to a better understanding of momentum transport caused by coherent structures. One of the challenges in experimental studies is obtaining detailed measurements of turbulence structures close to the wall. To facilitate this, Eckelmann [1], and Kreplin and Eckelmann [2] used oil as a working fluid in a channel flow with low Reynolds numbers so they could measure close to the wall (in wall units). Kim et al. [3] showed that direct numerical simulation (DNS) is a powerful tool to study turbulence in a channel flow at low Reynolds numbers. Since then, many DNS studies, often combined with conditional sampling, have provided detailed information about near wall coherent structures. Experimental investigation of Couette flow is more complicated than channel flow because a set-up with a moving wall is needed. A brief overview of experimental Couette flow investigations is given by Aydin and Leutheusser [4], who used a towing tank facility for their experiments. As can be expected from the no-slip velocity boundary

* Corresponding author. Present address: Sandia National Laboratories, 7011 East Ave., MS 9051, Livermore, CA 94550, USA. Tel.: +1-925-294-3833; fax: +1-925-294-2595.

*E-mail addresses:* bert@debusschere.net (B. Debusschere), rutland@engr.wisc.edu (C.J. Rutland).

0017-9310/$ - see front matter © 2003 Elsevier Ltd. All rights reserved.
doi:10.1016/j.ijheatmasstransfer.2003.10.031

**Nomenclature**

| | |
|---|---|
| $c_p$ | specific heat |
| $h$ | convective heat transfer coefficient |
| $k$ | molecular conductivity |
| $Nu$ | Nusselt number |
| $Pr$ | Prandtl number |
| $q$ | heat flux |
| $Re$ | Reynolds number |
| $T$, $t$ | instantaneous and fluctuating component of temperature |
| $t_\tau$ | friction temperature |
| $\overline{U_m}$ | mean streamwise velocity averaged over the cross section, bulk velocity |
| $U$, $u$ | instantaneous and fluctuating component of streamwise velocity |
| $u_\tau$ | friction velocity |
| $V$, $v$ | instantaneous and fluctuating component of wall-normal velocity |
| $W$, $w$ | instantaneous and fluctuating component of spanwise velocity |

*Greek symbols*

| | |
|---|---|
| $\delta$ | channel half-width |
| $\mu$ | dynamic viscosity |
| $v$ | kinematic viscosity |
| $\rho$ | fluid density |

*Subscripts*

| | |
|---|---|
| rms | root mean square |
| t | turbulent |
| w | at the wall |

*Superscript*

| | |
|---|---|
| – | averaged in $x$, $z$, and time |

conditions in channel and Couette flows, they found the near wall turbulence to be quite similar in both flows. This conclusion is also supported by Bech et al. [5] who studied Couette flow using data from both numerical simulation and physical experiments.

At the centerline however, the turbulence structure for channel and Couette flows is inherently different. In particular, the non-zero gradient in the mean velocity profile at the centerline of the Couette flow causes a non-zero production of turbulent kinetic energy. This effect is absent in the channel flow. As a result, the turbulent velocity fluctuations at the centerline of a Couette flow are considerably higher than in a channel flow [6]. Bech and Andersson [7] specifically investigated the behavior of the Reynolds shear stress at the centerline of plane Couette flow. They showed that mean shear generation and velocity–pressure gradient correlations play a crucial role in the generation and annihilation of the Reynolds shear stress. Strong, localized events at the centerline, with length scales of about the channel half-width, were essential in these generation and annihilation processes. Several simulations also reveal long streamwise vortical structures at the centerline of plane Couette flow. Komminaho et al. [8] reviewed several plane Couette flow studies in the literature for information regarding these long centerline structures. Because of their persistence, these structures require special attention in the choice of the domain sizes for the Couette flow.

Scalar transport in turbulent channel flows has been studied by Kim and Moin [9], who simulated passive scalar transport in a channel flow. Their analysis showed a strong similarity between the streamwise velocity and scalar fluctuations close to the wall. The scalar fluxes in the simulations of [9] are presented by Rogers, Mansour and Reynolds [10]. Lyons, Hanratty and McLaughlin [11] simulated a channel flow where the bottom wall was heated and the top wall was cooled at the same rate. At the centerline, this simulation showed a maximum in the turbulent temperature fluctuations, whereas the velocity fluctuations have a minimum at that location. This high level in the temperature fluctuations is a consequence of the production by the non-zero mean temperature gradient in the center of the domain. Using measurements in a channel flow with one wall at a constant temperature and the other wall at the ambient temperature, Teitel and Antonia [12] confirmed the findings of [11]. Scalar transport in Couette flow was studied by [13], although there has not been an investigation of the detailed transport mechanisms.

In the present work, simulations were performed of passive heat transfer in both plane channel and Couette flows. The main objective was to study the effect of the different velocity fields on the scalar transport. In all simulations, the Reynolds number, based on the bulk mean velocity and half the channel width was 3000. The walls were held at constant temperatures with one wall at a higher temperature than the other wall. From the comparisons, information was obtained about scalar transport mechanisms in both the near wall and the centerline area.

The next section gives more details about the cases that we studied and the numerics of the simulations. Then, the general characteristics of the channel and Couette cases are discussed, followed by a more detailed analysis of the scalar transport processes using statistical analysis and visualizations. The main conclusions are summarized at the end.

## 2. Numerical simulation parameters

Fig. 1 shows the geometry and main characteristics for the simulated plane channel and Couette flows. The flows were bounded in the $y$-direction by plates that were periodically infinite in the $x$- and $z$-directions. In the channel flow case, those plates were stationary but in the Couette flow, the upper wall moved at a velocity $2\overline{U_m}$ with respect to the lower wall, where $\overline{U_m}$ is the bulk mean velocity averaged over the cross section. In both cases, there was no internal heat generation. However, the walls were held at a constant temperature with the top wall at a higher temperature than the bottom wall, creating a heat flux $q$ from the top to the bottom.

In the simulations, the turbulent velocity and temperature fields were fully developed. To make the equations non-dimensional, all velocities were normalized by the mean velocity $\overline{U_m}$, and all lengths were normalized by the half-width $\delta$. Temperatures were normalized by the temperature difference between the walls. The Prandtl number was 0.7 and the density $\rho$ was fixed to 1. The Reynolds number in outer coordinates was

$$Re = \frac{\overline{U_m}\delta}{\nu} = 3000 \tag{1}$$

Based on the friction velocity $u_\tau$,

$$u_\tau = \sqrt{\frac{\tau_w}{\rho}} = \sqrt{\frac{\mu}{\rho}\left.\frac{\partial \overline{U}}{\partial y}\right|_{y=0}} \tag{2}$$

the Reynolds number ($Re_\tau = u_\tau\delta/\nu$) was 186 for the channel flow and 160 for the Couette flow. Both of these Reynolds numbers are in the fully turbulent flow regime and similar enough to have quantitatively comparable

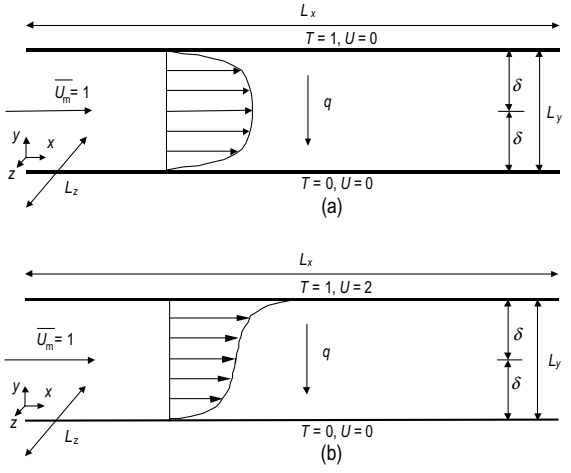


Fig. 1. Geometry and characteristics of the flows simulated in this study: (a) channel flow and (b) Couette flow.

turbulent statistics in the two flows. For use in normalizations, the wall friction temperature is defined as

$$t_\tau = \frac{q_w}{\rho c_p u_\tau} = \frac{k\left.\frac{\partial \overline{T}}{\partial y}\right|_{y=0}}{\rho c_p u_\tau} \tag{3}$$

For the channel flow in the present study, the wall friction temperature was 0.023. For the Couette flow, this value was higher at 0.033.

For the remainder of this text, all lengths are expressed in units of $\delta$. A bar over an upper case variable name denotes the average in $x$, $z$ and time of that variable, and the corresponding fluctuating quantity is given by the lower case variable name. For example,

$$U = \overline{U} + u \tag{4}$$

for the streamwise velocity. Except for the mean velocities and temperatures, all turbulent quantities shown in this text are normalized using the wall variables $u_\tau$ and $t_\tau$ as appropriate.

For the two cases shown in Fig. 1, the unsteady Navier–Stokes equations, together with the heat equation, were solved numerically using a DNS flow solver [14–16]. Assuming incompressible flow, a low Mach number approach [17] is used in this program to filter the acoustic waves from the flow field and allow for larger time steps. Periodic boundary conditions are used in the streamwise and spanwise directions, with no-slip walls in the $y$-direction. Spatial derivatives are calculated with sixth order accurate compact Pade schemes [18]. A third order accurate Runge Kutta method [19] is used for the time integration of the convection and diffusion terms in the Navier–Stokes equations. Using a time splitting technique, a Poisson equation for pressure is obtained. With a Fourier transformation in the $z$-direction and a cosine quarter wave transformation in the $y$-direction, this Poisson equation is reduced to a tri-diagonal system such that it can be solved non-iteratively. The grid is evenly spaced in all directions. In the non-periodic directions, however, half-cells are used at the boundaries where only the velocities and no pressures are calculated.

In choosing the domain sizes, special care was taken to resolve both the large and small length scales in the flows. For wall bounded turbulent flows, the largest turbulent flow structures are typically the near wall high and low speed streaks. These streaks can easily extend up to about a 1000 wall units in the streamwise direction. For simulations of Couette flow however, as mentioned in the introduction, the combination of velocity boundary conditions at the two walls has the side-effect that it allows large scale streamwise vortical structures to develop in the center of the domain. According to [8] an extremely long domain length of about $28\pi$ was needed to fully capture these vortices at a

Reynolds number of 750. Papavassiliou and Hanratty [20] interpreted these large scale structures as a secondary flow that is part of the mean velocity field. This secondary flow takes on the form of weak inviscid roll cells that receive energy from the Reynolds stresses and fill nearly the entire channel cross section. Even though this secondary flow is weak, it can have a significant impact on turbulent transport because the streamwise and wall-normal velocity components act in phase, and the flow is persistent in time and space. In the simulation of [20], the secondary flow accounted for up to 40% of the convective transport of streamwise momentum. It is likely though that in this study, the combination of periodic boundary conditions in the streamwise direction with a domain that was not long enough to let the structures decorrelate may have overemphasized the strength and persistence in time of this secondary flow.

Even though simulations suggest that these streamwise vortical structures are a strong feature in Couette flows, relatively little information about these structures can be found in experimental Couette flow literature. Bech et al. [5] experimentally observed streamwise vortical structures in a Couette flow between two counter-moving walls. More information was provided by Bottin et al. [21], who specifically investigated streamwise vortical structures in a transitional plane Couette flow, also between two counter-moving walls. From [21] it appears the vortical structures result from a flow instability in transitional Couette flow and are considered a key element in the transition to turbulence. Note that in both of these experiments, the structures were observed in Couette flows between counter-moving walls, which have a zero streamwise convective velocity near the centerline. In [21] the structures were purposely stabilized using a thin wire strung in the spanwise direction at the centerline. These experimental conditions may allow otherwise unstable structures to persist in the flow field.

In this respect, Andersson et al. [22] go as far as claiming that these structures have not been observed experimentally in the fully turbulent plane Couette flow regime and that they are a spurious flow phenomenon in numerical Couette flow simulations that use periodic boundary conditions in the streamwise direction. If the streamwise domain sizes are too small, these periodic boundary conditions provide a mechanism for self-amplification of elongated vortical structures, which allows those structures to develop into roll cells that fill the entire domain.

Regardless of whether or not these vortical structures appear in physical Couette flows, this secondary flow structure, which is stationary in time and space, is clearly an artifact of the geometry in Couette flows and will not show up in general turbulent flows with irregular geometries. Therefore, those structures are suppressed in this work by selecting a spanwise domain size of only 2 channel half-widths. In this way, the up- and downward motions of the streamwise roll cells cancel each other out in a box with periodic boundary conditions in the spanwise direction. By suppressing the large scale centerline vortices in a modified Couette flow with a narrow domain, this study is able to more clearly focus on the truly turbulent structures in the channel and Couette flows, representative of areas with low and high shear stress in general turbulent flows.

For both the channel and Couette flow cases described here, the domain size was $12\times2\times2$ with $231\times200\times64$ evenly spaced grid points in $x$, $y$, and $z$ respectively. These parameters gave a domain length of about 2000 wall units for both the channel and the Couette flow, with a spanwise width of 371 wall units for the channel flow and 320 wall units for the Couette flow. To verify whether all the large scales were resolved, autocorrelations were calculated for all velocity components and the temperature in both the streamwise and the spanwise directions (see for example Fig. 2). The autocorrelations in Fig. 2 at the centerline of the Couette flow show that the chosen domain width effectively suppresses the large scale streamwise structures that were observed by [8].

At the start of each simulation, the domain was initialized with a mean velocity profile, perturbed with random incompressible fluctuations in all directions. The flow was then allowed to develop for about $200\delta/\overline{U_{\mathrm{m}}}$. At this point, the turbulent flow was fully developed and the statistical sampling started. The time step in the calculations was chosen to be below a tenth of the viscous time scale $v/u_{\tau}^2$ such that individual events were accurately resolved. The temperature and flow field were sampled every $1\delta/\overline{U_{\mathrm{m}}}$. The total sampling time span was approximately $350\delta/\overline{U_{\mathrm{m}}}$, which was sufficient to reach statistical steady state with about 350 samples of the instantaneous flow and temperature fields in each

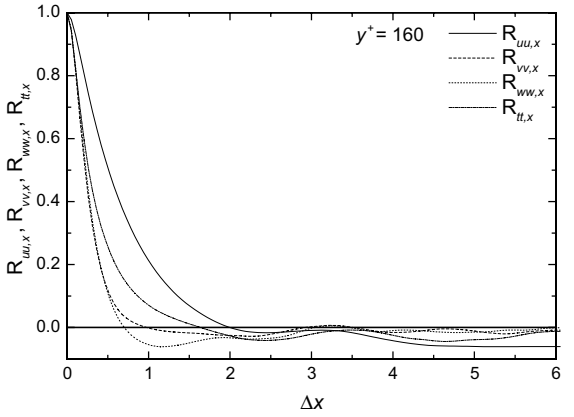


Fig. 2. Autocorrelations as a function of streamwise separation at the centerline of the Couette flow ($y^+ = 160$). Structures decorrelate before they reach half the domain length.

case. Using the homogeneous directions in the flow, statistical quantities were averaged over $x$, $z$ and time.

## 3. Results and discussion

### 3.1. General characteristics of the channel and Couette flows

This section highlights some of the general characteristics of the flows studied in this work (see also [15] for more details and for comparisons between the results from the present work and other computational and experimental work in the literature). Figs. 3 and 4 show the mean velocity and temperature profiles in outer coordinates for the channel and Couette flow. In the Couette flow, the velocity profile has been scaled by the velocity difference between the two walls to have the same range as the temperature profile. Both figures show a good symmetry between the upper and lower half of the domain, which indicates that the time averaging for the mean velocity and temperature has reached steady state. Note that the temperature and velocity profiles in the Couette flow are almost identical, due to the similarity in their boundary conditions. Also note that at the centerline, the mean temperature gradient in the channel flow is about twice the mean temperature gradient in the Couette flow (0.270 versus 0.137 respectively).

The root mean square values of the turbulent velocity and temperature fluctuations, normalized by $u_\tau$ and $t_\tau$, are shown in Figs. 5 and 6. Near the wall, the channel and the Couette case are very similar. Away from the wall, however, the profiles differ between the two cases. The channel flow has a higher level of temperature fluctuations but lower levels of turbulent velocity fluctuations than the Couette flow at the centerline. Later in this paper, we will show that the temperature fluctuations reach such a high level at the centerline of the channel flow because of packets of hot and cold fluid that come from the walls and collect near the centerline (see also [23]). The Couette flow has stronger turbulent velocity fluctuations throughout the domain and the temperature fluctuations behave more like the streamwise velocity fluctuations.

The turbulent Prandtl number, $Pr_t$, is shown in Fig. 7 for both the channel flow and the Couette flow. Near the wall, $Pr_t$ has a value close to one but the value drops to about 0.8 at the centerline. It is remarkable how well the turbulent Prandtl numbers agree between the present channel and Couette flow, despite the different velocity boundary conditions, as was also observed by [13]. The present turbulent Prandtl numbers also agree well with

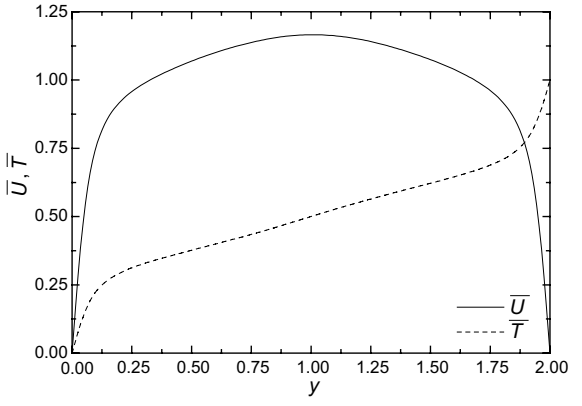


Fig. 3. Mean velocity and temperature profiles for the channel flow.

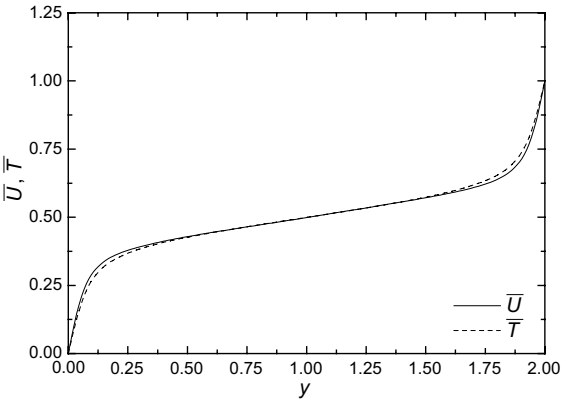


Fig. 4. Mean velocity and temperature profiles for the Couette flow. The velocity profile is scaled with the velocity difference between the top and the bottom wall to have the same range as the temperature profile.

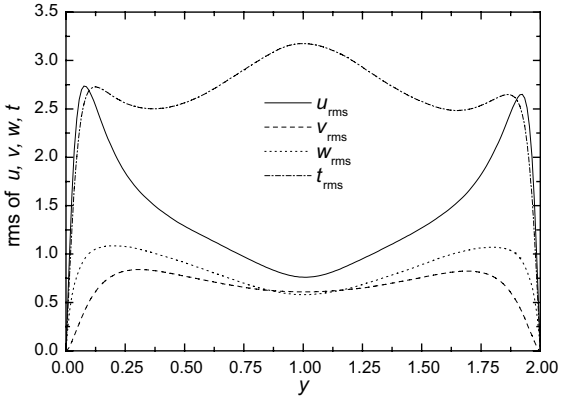


Fig. 5. Turbulent velocity and temperature fluctuations for the channel flow. The temperature fluctuations are strong at the centerline because of the non-zero production of temperature fluctuations at that location.

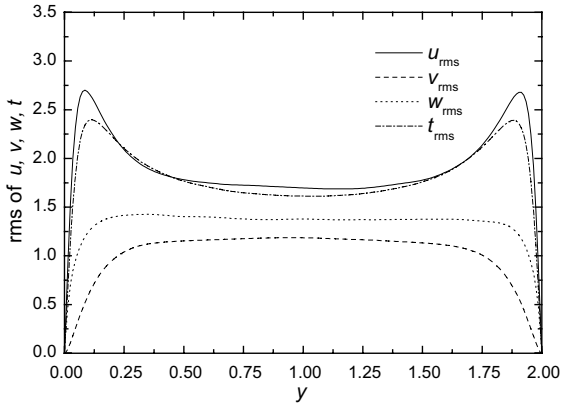


Fig. 6. Turbulent velocity and temperature fluctuations for the Couette flow. The temperature fluctuations at the centerline are lower but the velocity fluctuations are higher than in the channel flow at that location.

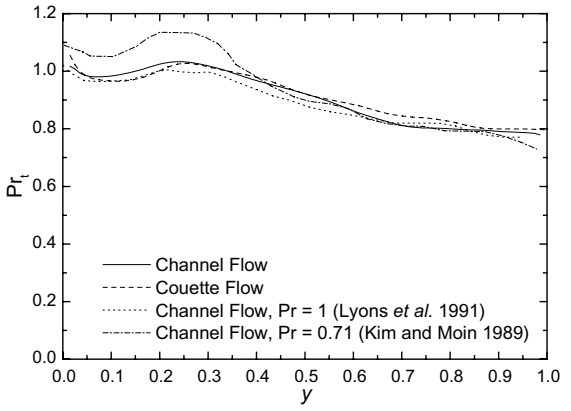


Fig. 7. The turbulent Prandtl number is similar in various simulations. Near the wall, $Pr_t$ is close to one but drops to about 0.8 at the centerline for all cases.

the channel flow simulations of [9,11] even though different boundary conditions were used for the temperature fields. In [11] one wall was heated and the other cooled at the same rate. In [9], heat was generated inside the domain and removed at the walls, which were both held at the same temperature.

The Nusselt number, defined as $Nu = h\delta/k$, is 6.08 for the channel flow in the present simulation. This value is similar to values found in the literature [11,24]. Page et al. [24] measured heat transfer in channel flows with the two walls at different but constant temperatures and a Prandtl number of 0.7. The Nusselt numbers derived from their data are $Nu = 6.27$ for $Re = 2245$ (run 45), and $Nu = 6.43$ for $Re = 2343$ (run 46). In a simulation of channel flow at $Re = 2262$, with constant heat flux boundaries and a Prandtl number of 1, Lyons et al. [11] found a Nusselt number of $Nu = 6.34$. For the Couette flow in the present simulation, the Nusselt number is $Nu = 7.30$, which is about 20% higher than the Nusselt number of 6.08 for the channel flow. As will be explained later on, the Couette flow has better turbulent heat transfer mechanisms in the center of the domain, resulting in an overall more efficient heat transfer between the two walls.

### 3.2. Near wall heat transfer mechanisms

The steady-state thermal energy equation (5) expresses the temperature balance for an infinitesimal control volume. The terms of this equation are plotted in Figs. 8 and 9 with their signs in Eq. (5) so that positive values represent addition of heat to a control volume and negative values represent heat loss.

$$-u\overline{\frac{\partial t}{\partial x}} - v\overline{\frac{\partial t}{\partial y}} - w\overline{\frac{\partial t}{\partial z}} + \frac{1}{RePr}\frac{\partial^2 \overline{T}}{\partial y^2} = 0 \tag{5}$$

All terms in Figs. 8 and 11 have been scaled by $u_\tau^2 t_\tau Re$. Near the wall, all terms in Eq. (5) are similar in the two cases. For $y < 0.25$ molecular transport removes energy from a control volume because the temperature gradient becomes steeper close to the wall. This effect is primarily balanced by the term $-\overline{w\partial t/\partial z}$, which corresponds to a convective transport by near wall streamwise vortices (see also discussion of Figs. 10 and 11). Further away from the wall, all terms in Eq. (5) are small relative to their near wall values. In the Couette flow, all terms tend to vanish towards the center of the domain. In the channel flow, the terms $-\overline{u\partial t/\partial x}$ and $-\overline{w\partial t/\partial z}$ remain non-zero up to the centerline and balance each other.

As stated above, Figs. 8 and 9 show a significantly different behavior for the terms of the thermal energy

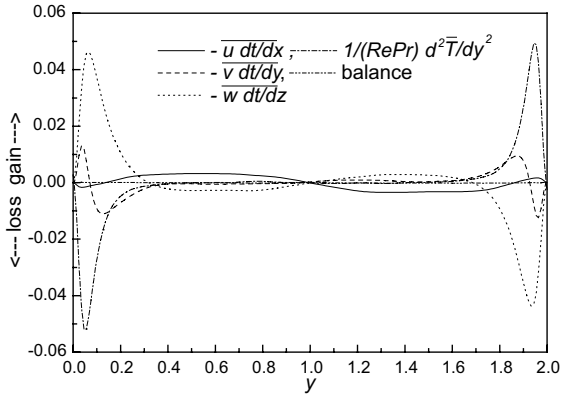


Fig. 8. Thermal energy balance for the channel flow (Eq. (5)): near the wall, the increase in molecular transport is balanced by $-\overline{w\partial t/\partial z}$. Away from the wall, the $-\overline{u\partial t/\partial x}$ term is balanced by $-\overline{w\partial t/\partial z}$.

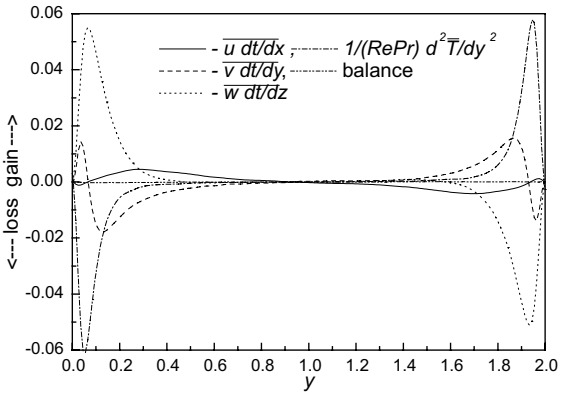


Fig. 9. Thermal energy balance for the Couette flow (Eq. (5)): near the wall, molecular transport is balanced by $-\overline{w\partial t/\partial z}$. Away from the wall, all terms vanish towards the center of the domain.

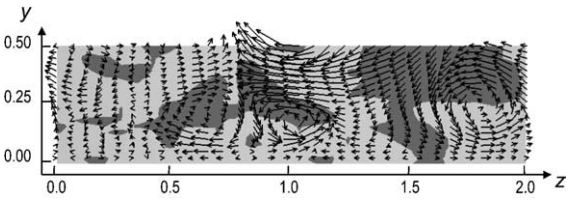


Fig. 10. Instantaneous velocity vectors and filled contours of $-w\partial t/\partial z$ in a cut normal to the streamwise direction in the near wall region of the Couette flow. The mean flow goes into the page. Regions where $-w\partial t/\partial z < 0$ are colored dark gray, regions where $-w\partial t/\partial z > 0$ are colored light gray. Streamwise vortices around $y \approx 0.2$, $z = 0.8$ and $z = 1.8$ move heat towards the wall.

equation (5) between the regions "near the wall" and regions "further away from the wall". The energy equation terms change rapidly between $y \approx 0.2$ and $y \approx 0.3$. Below, it will be shown that vortices, centered around $y \approx 0.2$ accommodate this transition in heat transfer mechanisms. Fig. 10 shows the turbulent velocity vectors in a plane normal to the streamwise direction, near the lower wall of the domain. The picture was made for the Couette flow, but near the wall, the results for the channel flow are similar.

The background of this figure is colored according to the value of $-w\partial t/\partial z$, which in Eq. (5) corresponds to the convective heat transfer term that offsets the increased heat loss due to molecular conduction near the wall. Fig. 10 shows a pair of counter-rotating streamwise vortices around $y = 0.2$, $z = 0.8$ and a single streamwise vortex around $y = 0.25$, $z = 1.8$. The sign of $-w\partial t/\partial z$ changes from negative to positive as fluid moves below the centers of the vortices. This sign change indicates that the vortices extract heat from the fluid away from the wall and give off heat to the fluid closer to the wall.

To verify that the near wall streamwise vortices are indeed responsible for the behavior of $-\overline{w\partial t/\partial z}$ (and similarly $-\overline{v\partial t/\partial y}$), conditional averaging over $x$ and time was performed in $yz$-planes with significant $-w\partial t/\partial z$ events near the wall. Fig. 11 shows the results of this conditional averaging for the Couette flow. Only the $yz$-planes that have $-w\partial t/\partial z \geqslant -\overline{w\partial t/\partial z}$ and $w < 0$ at the point in the middle of the spanwise dimension where $-\overline{w\partial t/\partial z}$ reaches a maximum in $y$ (see Fig. 9) are included in the sampling. Note that since all $yz$-planes are considered for sampling, some events may be counted several times. All conditionally averaged quantities $\phi$ are denoted as $\langle\phi\rangle$. Again, for the channel flow, all results for this conditional averaging are very similar to the Couette flow. The conditionally averaged temperature in Fig. 11 is normalized by the friction temperature $t_\tau$. The terms $\langle -v\partial t/\partial y\rangle$ and $\langle -w\partial t/\partial z\rangle$ are normalized by $u_\tau^2 t_\tau Re$.

The conditionally averaged velocity field, represented by the vectors in Fig. 11 confirms that a rotating structure, centered around $y \approx 0.2$ is indeed associated with strong $-w\partial t/\partial z$ events near the wall. At $y \approx 0.1$, the fluid that is pushed down by this vortex is significantly warmer than the local average due to the strong curvature of the mean temperature profile in that area. As a result, $\langle -v\partial t/\partial y\rangle$ is negative in this area, as shown by the dark area in Fig. 11c, which matches the negative area for $-\overline{v\partial t/\partial y}$ in Fig. 9. As the fluid is swept along the wall by the vortex, it gives off heat by molecular conduction. In Fig. 11b, this shows up as an area of positive $\langle -w\partial t/\partial z\rangle$ between the wall and the center of the vortex, which matches the area of positive $-\overline{w\partial t/\partial z}$ in Fig. 9. Note in Fig. 11c that very close to the wall, $\langle -v\partial t/\partial y\rangle$ becomes positive as well, because the fluid that is convected downward gives off heat by molecular conduction towards the wall. This is also consistent with Fig. 9.

Overall, in the near wall area, the streamwise vortices compensate for the heat lost by the increased molecular conduction in that area. In this way, the streamwise vortices accommodate the transition between the area away from the wall, where convective heat transfer $-vt$ is the main heat transfer mechanism, to the area near the wall, where conductive heat transfer dominates.

### 3.3. Heat transfer in the centerline area

Near the centerline, the heat transfer is significantly different in the channel and Couette flows, as would be expected from the differences in the turbulence fields between the two flows at that location. Figs. 12 and 13 show two-dimensional temperature correlations calculated at the centerline ($y = 1$) for both the channel and

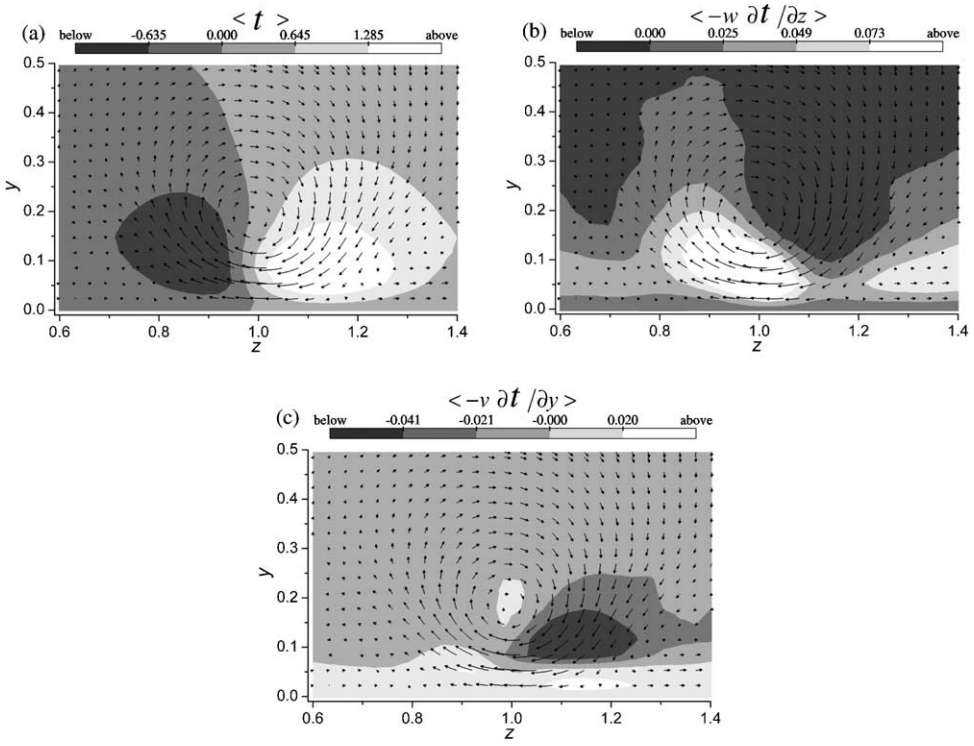


Fig. 11. Conditional sampling of $-w\partial t/\partial z$ events in the near wall region of the Couette flow: $0 < y < 0.5$, $0.6 < z < 1.4$. Only $yz$-planes where $-w\partial t/\partial z \geqslant -\overline{w\partial t/\partial z}$ and $w < 0$ at $y = 0.07$ and $z = 1.0$ are averaged. The vectors show the conditionally averaged velocity field and the contours represent the conditional averages of (a) fluctuating temperature $\langle t\rangle$, (b) $\langle -w\partial t/\partial z\rangle$, and (c) $\langle -v\partial t/\partial y\rangle$. The velocity field reveals a near wall rotating structure and the signs of $\langle -w\partial t/\partial z\rangle$ and $\langle -v\partial t/\partial y\rangle$ correspond to the terms in Fig. 9. For clarity of the vector plot, only every 3rd point in $y$ is shown.

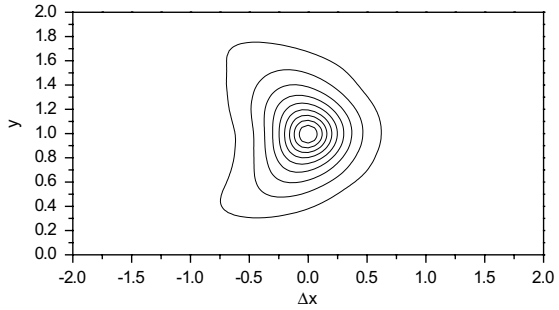


Fig. 12. Two-dimensional temperature correlations in the $xy$-plane for the channel flow. The contour level values go down monotonically from 0.9 in the center to 0.1 at the outside. The temperature at the center correlates with near wall events, which are trailing with respect to the center.

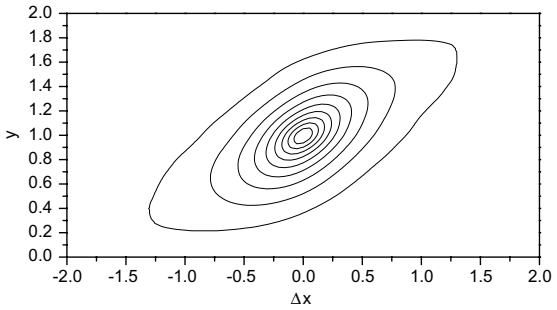


Fig. 13. Two-dimensional temperature correlations in the $xy$-plane for the Couette flow. The contour level values go down monotonically from 0.9 in the center to 0.1 at the outside. The temperature at the center correlates with near wall events, which are trailing (bottom wall) or ahead (top wall) with respect to the center. The overall correlation is stronger in the Couette flow than in the channel flow.

the Couette flow. For ease of notation, these correlations are calculated as:

$$R_{t,xy}(\Delta x, y) = \frac{\overline{t(x,1,z)t(x+\Delta x, y, z)}}{t_{\mathrm{rms}}(1)t_{\mathrm{rms}}(y)} \tag{6}$$

where the overbar denotes averaging in $x$, $z$, and time.

For both the channel and Couette flow, the two-dimensional correlations show that the temperature at the centerline correlates with the temperature near the walls. In the channel flow, near wall events from both

walls are trailing with respect to the centerline, shaping the temperature correlation in Fig. 12 like an arrowhead. However, in the Couette flow, events near the top wall are moving faster than the centerline, giving the correlation in Fig. 13 more the shape of a stretched ellipsoid. More importantly, in the Couette flow the autocorrelation remains above zero closer to the walls than in the channel flow. This higher correlation between near wall and centerline temperature events suggests the existence of stronger structures in the Couette flow that transport heat between the walls across the centerline.

Evidence of such structures can also be found in visualizations of instantaneous flow fields. For example, Fig. 14 compares filled contours of the fluctuating temperature for the channel and the Couette flow. The plane shown is normal to the spanwise direction at $z = 0$ and spans the full streamwise and normal dimensions of the domain. The mean flow is from left to right and all temperatures have been normalized by the friction temperature $t_\tau$.

In the fluctuating temperature contours of Fig. 14, many structures show up as streaky regions that are either dark gray (fluid colder than the local mean temperature) or white (fluid warmer than the local mean). When followed in time, these structures typically start at the wall, then grow and eventually separate off the wall. As the structures move away from the wall, they are convected along with the mean flow. In the channel flow (Fig. 14a), all structures are moving to the right as they move towards the centerline. Therefore, structures coming from the top and the bottom wall propagate in angles such that they cross at the centerline. These

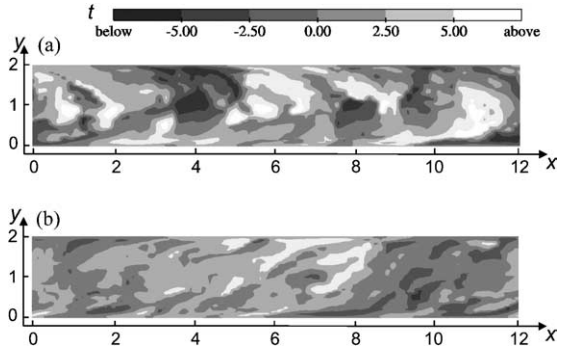


Fig. 14. Comparison of the fluctuating components of temperature between the two flows. (a) Channel flow: structures coming from the top and the bottom wall propagate in different directions and do not cross the centerline so that packets of hot and cold fluid form along the centerline. (b) Couette flow: structures coming from the top and bottom wall are aligned across the centerline. The level of temperature fluctuations near the centerline is lower than in the channel flow.

structures do not move across the centerline because the turbulence levels are low in that area. As a result, the hot or cold fluid that is carried with these structures tends to stay at the centerline. In this way, large packets of hot and cold fluid form that are convected along with the main flow, consistent with the high levels of turbulent temperature fluctuations at the channel centerline, as shown in Fig. 5. The shapes and sizes of these hot and cold spots near the centerline are also consistent with the two-dimensional temperature correlations in Fig. 12.

In the Couette flow however (Fig. 14b), the structures coming off the upper, moving wall are trailing with respect to that wall. Therefore, structures separating from both walls move along the same slope relative to the mean flow. Sometimes, structures even connect with each other at the centerline and form stretched temperature streaks going all the way from one wall to the other (for example, the dark gray streak going from $x \approx 8$ at the bottom wall to $x \approx 11$ at the top wall). The sizes and shapes of these structures again strongly resemble the two-dimensional temperature correlations in Fig. 13. Because the normal gradients of the mean velocity and temperature are always positive in the Couette flow, a fluid packet with $u < 0$ and $t < 0$ that moves up from the lower wall will keep receiving momentum and energy from the mean velocity enabling it to cross the centerline. In the channel flow, however, structures that move to the centerline can not extract momentum from the mean velocity field and tend to remain there and decay.

Because turbulent structures can cross the centerline in the Couette flow, hot or cold fluid that is moving along with these structures can easily cross the centerline and there is no concentration of hot or cold fluid packets at that location. Thus, the more efficient heat transfer across the centerline of the Couette flow reduces the level of temperature fluctuations in that area.

## 4. Conclusions

In this study, simulations were performed of a channel and a Couette flow with passive heat transfer to investigate turbulent scalar transport. The domain size of these cases has been chosen to resolve all relevant turbulent length scales, but at the same time suppress large scale secondary flows in the Couette flow case. The results of the simulations were studied using statistical analysis of transport equations, two-dimensional correlations, as well as flow visualization.

The turbulent Prandtl number for both simulations has a value close to one near the wall and decreases to about 0.8 at the centerline. The profile for $Pr_t$ is very similar in both simulations as well as in other studies in the literature.

Near the wall, both the momentum and heat transfer characteristics are very similar in the channel and the Couette flow. Using conditional sampling, it was shown that streamwise vortices centered around $y \approx 0.2$ carry heat into the near wall region and accommodate the transition from convective to conductive heat transfer in this area.

Away from the wall, the channel and Couette flow have different characteristics because the Couette flow has a non-zero mean velocity gradient in the wall-normal direction at the centerline. Due to this gradient, the Couette flow has significant turbulence production near the centerline, which results in higher turbulence levels than in the channel flow. Consistent with this higher turbulence, large scale turbulent motions exist in the Couette flow that reach across the centerline and transport heat from the one wall to the other. In the channel flow, the turbulence is much weaker near the centerline and structures do not cross the centerline. Packets of hot or cold fluid form at the centerline from fluid that came from the walls. Those packets convect along with the mean flow, causing high fluctuating temperature levels at the channel centerline.

Overall, the Couette flow has more efficient heat transfer between the two walls, resulting in a Nusselt number that is about 20% higher than in the channel flow for the same Reynolds number.

## Acknowledgements

The research for this paper was supported by the National Science Foundation (grant no. CTS-9358419) and by the Engine Research Center of the University of Wisconsin, Madison. Computer time was granted by Cray Research, Inc. We would also like to thank Dr. T.M. Al-Shalaan and Dr. S.D. Mason for the use of their CFD codes, and Prof. K.A. Thole for the helpful discussions and suggestions.

## References

[1] H. Eckelmann, The structure of the viscous sublayer and the adjacent wall region in a turbulent channel flow, J. Fluid Mech. 65 (3) (1974) 439–459.
[2] H.P. Kreplin, H. Eckelmann, Behavior of the three fluctuating velocity components in the wall region of a turbulent channel flow, Phys. Fluids 22 (7) (1979) 1233–1239.
[3] J. Kim, P. Moin, R. Moser, Turbulence statistics in fully developed channel flow at low Reynolds number, J. Fluid Mech. 177 (1987) 133–166.
[4] E.M. Aydin, H.J. Leutheusser, Plane-Couette flow between smooth and rough walls, Exp. Fluids 11 (1991) 302–312.
[5] K.H. Bech, N. Tillmark, P.H. Alfredsson, H.I. Andersson, An investigation of turbulent plane Couette flow at low Reynolds numbers, J. Fluid Mech. 286 (1995) 291–325.
[6] M.M.M. El Telbany, A.J. Reynolds, The structure of turbulent plane Couette flow, Trans. ASME J. Fluids Eng. 104 (1982) 367–372.
[7] K.H. Bech, H.I. Andersson, Structure of Reynolds shear stress in the central region of plane Couette flow, Fluid Dyn. Res. 18 (1996) 65–79.
[8] J. Komminaho, A. Lundbladh, A.V. Johansson, Very large structures in plane turbulent Couette flow, J. Fluid Mech. 320 (1996) 259–285.
[9] J. Kim, P. Moin, Transport of passive scalars in a turbulent channel flow, in: J.-C. Andre et al. (Eds.), Turbulent Shear Flows, vol. 6, Springer-Verlag, Berlin, 1989, pp. 85–96.
[10] M.M. Rogers, N.N. Mansour, W.C. Reynolds, An algebraic model for the turbulent flux of a passive scalar, J. Fluid Mech. 203 (1989) 77–101.
[11] S.L. Lyons, T.J. Hanratty, J.B. McLaughlin, Direct numerical simulation of passive heat transfer in a turbulent channel flow, Int. J. Heat Mass Transfer 34 (4/5) (1991) 1149–1161.
[12] M. Teitel, R.A. Antonia, Heat transfer in fully developed turbulent channel flow: comparison between experiment and direct numerical simulations, Int. J. Heat Mass Transfer 36 (6) (1993) 1701–1706.
[13] H. Kawamura, H. Abe, K. Shingai, DNS of turbulence and heat transport in a channel flow with different Reynolds and Prandtl numbers and boundary conditions, in: Y. Nagano, K. Hanjalić, T. Tsuji (Eds.), 3rd Int. Symp. on Turbulence, Heat and Mass Transfer, Aichi Shuppan, 2000, pp. 15–32.
[14] T.M. Al-Shaalan, Studying reacting turbulent Couette flow using direct numerical simulations, PhD Thesis, University of Wisconsin, Madison, WI, 1997.
[15] B. Debusschere, Turbulent scalar transport in non-reacting and reacting flows, PhD Thesis, University of Wisconsin, Madison, WI, 2001.
[16] S.D. Mason, Turbulence transport in spatially developing reacting shear layers, PhD Thesis, University of Wisconsin, Madison, WI, 2000.
[17] P.A. McMurtry, W.-H. Jou, J.J. Riley, R.W. Metcalfe, Direct numerical simulations of a reacting mixing layer with chemical heat release, AIAA 23rd Aerospace Sciences Meeting, Reno, NV, AIAA-85-0143, 1985.
[18] S.K. Lele, Compact finite difference schemes with spectral-like resolution, J. Comput. Phys. 103 (1) (1992) 16–42.
[19] H. Le, P. Moin, An improvement of fractional step methods for the incompressible Navier–Stokes equations, J. Comput. Phys. 92 (2) (1991) 369–379.
[20] D.V. Papavassiliou, T.J. Hanratty, Interpretation of large-scale structures observed in a turbulent plane Couette flow, Int. J. Heat Fluid Flow 18 (1) (1997) 55–69.
[21] S. Bottin, O. Dauchot, F. Daviaud, P. Manneville, Experimental evidence of streamwise vortices as finite amplitude solutions in transitional plane Couette flow, Phys. Fluids 10 (10) (1998) 2597–2607.
[22] H.I. Andersson, M. Lygren, R. Kristoffersen, Roll cells in turbulent plane Couette flow: reality or artifact?, in: Proceedings of the Sixteenth International Conference on Numerical Methods in Fluid Dynamics, Springer-Verlag, Berlin, 1998, pp. 117–122.

[23] P.M. Wikström, A.V. Johansson, DNS and scalar-flux transport modeling in a turbulent channel flow, in: Proceedings of the 2nd EF Conference in Turbulent Heat Transfer, Manchester, UK, vol. 1, 1998, pp. 6.46–6.51.

[24] F. Page Jr., W.G. Schlinger, D.K. Breaux, B.H. Sage, Point values of eddy conductivity and viscosity in uniform flow between parallel plates, Ind. Eng. Chem. 44 (2) (1952) 424–430.